Effect of speckles on the depth sensitivity of laser Doppler perfusion imaging

V. Rajan, B. Varghese, T. G. van Leeuwen and W. Steenbergen

Institute for Biomedical Technology BMTI, Biophysical Engineering Group, University of Twente, P.O. Box 217, NL-7500AE Enschede, The Netherlands.
v.rajan@tnw.utwente.nl

Abstract: A theoretical model is presented and experimentally validated that allows the prediction of the effect of speckles on the depth sensitivity of laser Doppler perfusion imaging. It is shown that the influence of speckles on depth sensitivity is large. In particular the sensitivity to particle motion in superficial layers is strongly beam diameter dependent: decreasing the beam diameter on the tissue surface increases the sensitivity to superficial motion to a much stronger extent than sensitivity to motion at a larger depth. This can be explained through the effect of beam diameter changes on the fractional coherence areas generated by photons with different penetration depths in the tissue.

OCIS codes: (170.3340) Laser Doppler velocimetry; (170.1650) Coherence imaging; (170.3660) Light propagation in tissues; (290.1350) Backscattering.

References and links

1. K. Wårdell, A. Jakobsson, and G. E. Nilsson, "Laser Doppler perfusion imaging by dynamic light scattering," IEEE Trans. Biomed. Eng. **40**, 309-316 (1993).
2. T. J. H. Essex and P. O. Byrne, "A laser Doppler scanner for imaging blood flow in skin," J. Biomed. Eng. **13**, 189-193 (1991).
3. V. Rajan, B. Varghese, T. G. van Leeuwen, and W. Steenbergen, "Speckles in Laser Doppler Perfusion Imaging," Opt. Lett. **31**, 468-470 (2006).
4. A. Jakobsson and G. E. Nilsson, "Prediction of sampling depth and photon pathlength in laser Doppler flowmetry," Med. Biol. Eng. Comput. **31**, 301–307 (1993).
5. E. J. Droog, W. Steenbergen and F. Sjöberg, "Measurement of depth of burns by laser Doppler perfusion imaging," Burns **27,** 561–568 (2001).
6. W. Eichhorn, T. Auer, E. D. Voy, and K. Hoffmann "Laser Doppler imaging of axial and random pattern flaps in the maxillo-facial area. A preliminary report," J Craniomaxillofac Surg. **22,** 301-306 (1994).
7. A. Serov, W. Steenbergen, and F. F. M. de Mul, "Prediction of the photodetector signal generated by Doppler-induced speckle fluctuations: theory and some validations," J. Opt. Soc. Am. A **18**, 622-630 (2001).
8. V. Rajan, B. Varghese, T. G. van Leeuwen, and W. Steenbergen, "Quantification of spatial intensity correlations and photodetector intensity fluctuations of coherent light reflected from turbid particle suspensions," Phys. Rev. E **75,** 060901-4 (2007).
9. F. F. M. de Mul, M. H. Koelink, M. L. Kok, P. J. Harmsma, J. Greve, R. Graaff, and J. G. Aarnoudse, "Laser Doppler velocimetry and Monte Carlo simulations on models for blood perfusion in tissue," Appl. Opt. **34**, 6595-6611 (1995).
10. A. Kharine, S. Manohar, R. Seeton, R. G. M. Kolkman, R. A. Bolt, W. Steenbergen, F. F. M de Mul "Poly(vinyl alcohol) gels for use as tissue phantoms in photoacoustic mammography," Phys. Med. Biol. **48,** 357–370 (2003).
11. J. C. Hebden, B. D Price, A. P. Gibson and G. Royle, "A soft deformable tissue-equivalent phantom for diffuse optical tomography," Phys. Med. Biol. **51,** 5581-5590 (2006).
12. A. Fullerton, B. Rode, and J. Serup, "Skin irritation typing and grading based on laser Doppler perfusion imaging," Skin Res. Technol. **8**, 23–31 (2002).

1. Introduction

Laser Doppler perfusion imaging (LDPI) [1, 2] is a non-invasive technique to measure blood flow maps on an area of tissue. The photodetector signal generated in a laser Doppler perfusion instrument can be considered to be generated by a large number of dynamic speckles (coherence areas). It has been shown [3] that the scattering level of the tissue strongly affects a laser Doppler imager signal due to the varying number of coherence areas

#83991 - $15.00 USD Received 11 Jun 2007; revised 9 Aug 2007; accepted 13 Aug 2007; published 15 Aug 2007

involved in the detection. Variations in absorption as well as the diameter of the illuminating beam will have similar influence on LDPI-readings through the number of coherence areas. Figure 1 shows the speckle pattern generated by a narrow (e^{-2} beam diameter, 0.5mm) and a wide beam (e^{-2} beam diameter, 4mm) illuminating a water suspension of Polystyrene microspheres (Polysciences Inc) of 0.771 μm diameter (scattering anisotropy g=0.9)

Tissue optical properties also will affect the depth sensitivity of a laser Doppler system. The depth sensitivity here is defined as the sensitivity of the instrument to motion of particles at a certain depth under the illuminated surface of the turbid medium. The decay of the depth sensitivity due to the limited penetration depth of photons is an obvious phenomenon [4]. However, in this paper we demonstrate that, apart from photon penetration depth statistics, the speckle phenomenon has an independent influence on the depth sensitivity. In order to correctly interpret the perfusion signal it is important to know the sensitivity of the instrument to motion at different depths. This is particularly important when we assess the burn depth [5] and perfusion of a grafted skin flap [6]. In this paper we experimentally investigate the depth sensitivity of the laser Doppler perfusion imager. In addition we predict the influence of coherence areas on LDPI depth sensitivity by a theoretical model.

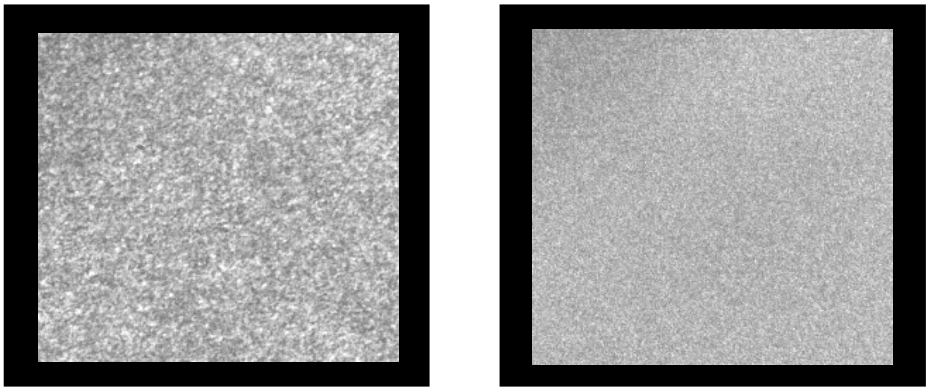

Fig.1. Speckle pattern of light diffusely reflected from a scattering medium which is illuminated with a narrow (to the left, 2.51 MB file, A) and a broad beam (to the right, 2.49 MB file, B). Please see also the movies.

The fundamental output quantities of a laser Doppler instrument are the moments of the power spectra of photodetector intensity fluctuations. M_1, the first moment is regarded to be proportional to the flux of the moving scatterers (also called the perfusion) and M_0, the zero order moment is considered to be proportional to the concentration of moving scatterers. These moments of the power spectrum depend on the spectral width and the modulation depth of the photodetector signal. The latter quantity in turn is related to the amount of coherence areas. When all photons are Doppler shifted, the zero order moment, normalized with the DC^2 signal can be written as [7]

$$\frac{M_0}{DC^2} = \frac{< i_{ac}^2 >}{\langle i_{dc} \rangle^2} \propto \frac{1}{N} \tag{1}$$

where $\left\langle i_{AC}^2 \right\rangle$ is the mean square of the photocurrent fluctuations, $\left\langle i_{DC} \right\rangle$ the mean photocurrent, and *N* the number of speckles on the detector. So any change in the amount of coherence areas *N* will influence the laser Doppler perfusion estimate. For a given photodetector size, the amount of speckles (coherence areas) depends on the average coherence area which is roughly dependent on the solid angle at which the photons attack on the detector. Changes in optical properties result in photon trajectories through the medium which make photons to escape from the tissue at different distances from the source. So the solid angle generated by the back scattered photons on the detector changes with optical properties, which changes the average

#83991 - $15.00 USD Received 11 Jun 2007; revised 9 Aug 2007; accepted 13 Aug 2007; published 15 Aug 2007

coherence area. This situation is illustrated in Fig. 2 where two solid angles Ω_1 and Ω_2 are shown, which might be associated with narrow and wide illuminating beams, respectively. Figure 1 clearly shows this coherence area variation with illuminating beam diameter.

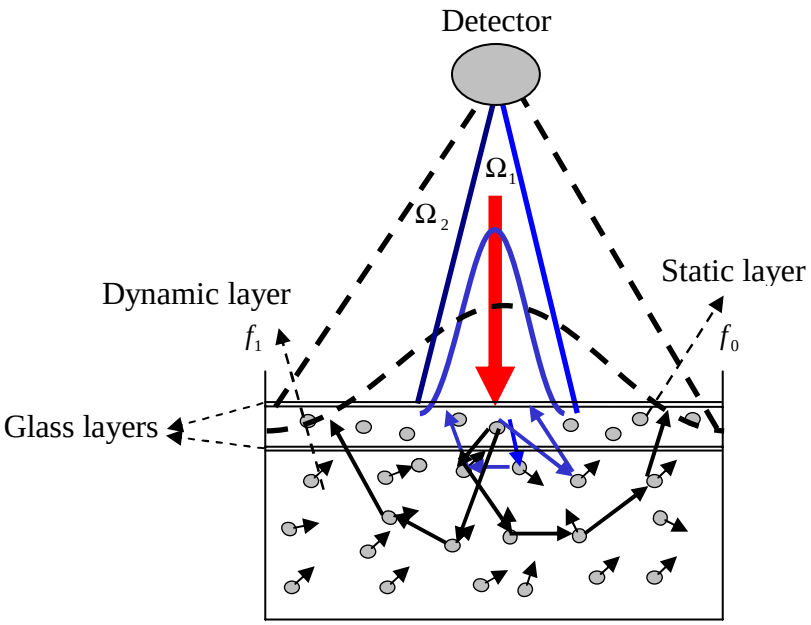

Fig. 2. Schematic of optical scattering phantom with static and dynamic layers. Solid lines represent the back scattered intensity distribution and dashed line represents the solid angle generated on the detector by photons traveled superficially and deep.

Earlier we reported [8] on the influence of optical properties on the average coherence area, quantitatively, in an optical configuration used in laser Doppler perfusion imaging. It was observed that with a typical beam diameter of 0.5mm the average coherence area on the detector varies by a factor of 4 when the reduced scattering coefficient varied from 0.5mm^{-1} to 4.0mm^{-1}. This variation drops to a factor of 1.5 when the beam diameter is increased to 4.0mm. This shows the influence of the reduced scattering coefficient on the coherence area which in turn influences the response of the laser Doppler system to the same perfusion level under different optical surroundings.

The coherence area is also influenced by the depth probed by the photons. Photons traveling deep into a scattering medium generate wider intensity patterns in leaving the medium and therefore generate smaller coherence areas (Fig. 2). This reduces the relative contribution of these photons in the total flux signal. Therefore in this optical situation the effect of coherence area is not merely a change in the total system response but also a change in the depth sensitivity of the instrument. In this paper we present and validate a theoretical approach to quantitatively assess the system's response to motion at different depths.

2. Theory

Recently we showed [8] that the spatial correlations of the intensity of far field dynamic speckle patterns generated by mixed static and dynamic turbid media illuminated by coherent light can be predicted. For that we used a theoretical /computational frame work which can model the variance of photocurrent fluctuations on a far-field detector collecting back-scattered photons on the basis of Monte Carlo derived photon statistics, taking in to account the speckle phenomenon.

#83991 - $15.00 USD Received 11 Jun 2007; revised 9 Aug 2007; accepted 13 Aug 2007; published 15 Aug 2007

The photocurrent mean square intensity fluctuations can be expressed in terms of coherence areas formed by different fractions of Doppler shifted photons,

$$< i_{ac}^2 >= A_{\det} R^2 \langle I \rangle^2 \left[2 f_0 f_1 A_{coh}^{01} + f_1^2 A_{coh}^{11} \right] \quad (2)$$

where $A_{\det}$ is the effective detection area, R is the responsivity of the detector and $< I >$ is the average intensity of the light within the detection area. Furthermore f_0 is the fraction of non-Doppler shifted photons, f_1 is the fraction of Doppler shifted photons (f_1 =1- f_0) A_{coh}^{01} is the fractional coherence area formed by the interference of Doppler shifted photons with non-Doppler shifted photons, and A_{coh}^{11} is the fractional coherence area formed by only Doppler shifted photons. These fractional coherence areas can be calculated by Fourier-transforming the respective Monte Carlo predicted intensity distributions of these photon fractions according to the Van Cittert Zernike theorem and a simple integration of the resulting spatial field coherence functions $\gamma_{EE}(\Delta x)$ according to

$$A_{coh}^{ij} = 2\pi \int_0^\infty \gamma_{EE}^{j}(\Delta x) \gamma_{EE}^{*j}(\Delta x) \Delta x d\Delta x \quad (3)$$

with *I* and *j* appearing in the same combinations and with the same meaning as in Eq. (2).

Equations (2) and (3) give the mean square value of photocurrent fluctuations in terms of correlation functions of one group of unshifted photons and one group of Doppler shifted photons. This will occur in, for instance, media like skin which, depending on the optical properties of the tissue matrix, and the blood volume, will reflect photons with nonzero and zero Doppler shift. By normalizing with $\langle i_{dc} \rangle = R \langle I \rangle A_{\det}$ the photodetector signal modulation depth can be written as,

$$\frac{< i_{ac}^2 >}{\langle i_{dc} \rangle^2} = \frac{\left[2 f_0 f_1 A_{coh}^{01} + f_1^2 A_{coh}^{11} \right]}{2 A_{\det}} \quad (4)$$

With Eqs. (3) and (4) we can predict the signal modulation depth theoretically if we have the intensity distribution on the tissue surface of the Doppler shifted and non-Doppler shifted photons and their fractions f_1 and f_0. Here a factor of 2 is introduced in the denominator, since a non-polarized speckle pattern is a summation of two independent orthogonally polarized patterns which are formed by multiple scattering. Since the Monte Carlo method [9] can simulate the photon intensity distribution from an optical medium and provide the statistics of the detected photons, it can give input parameters to calculate the fractional coherence areas on the photodetector, and in turn we can predict the signal modulation depth.

3. Materials and methods

Phantoms two layered are made: the top layer which is static, and a bottom layer which is dynamic. A schematic of the scattering phantom is shown in Fig. 2. Both layers are prepared with a reduced scattering coefficient $\mu_s' = 2mm^{-1}$, a scattering anisotropy g=0.9 and an absorption coefficient of $\mu_a = 0.02mm^{-1}$. The dynamic scattering phantom is made of polystyrene microspheres ∅ 0.771 μm mixed with water. Ecoline Black ink (Royal Talens) is added to get the desired absorption. The self-diffusion coefficient of the particles in Brownian motion is calculated as, $D_B = K_B T / 3\pi\eta a$ =5.56*10^{-9} cm^2/s (Stokes-Einstein relation). Here K_B is the Boltzmann constant, T is the temperature (293 K), η is the viscosity of the suspending liquid [η =1.0 cps for water] and a is the hydrodynamic diameter (∅0.77 μm) of the scattering particles. From this the expected single-scattering correlation time (the inverse

#83991 - $15.00 USD Received 11 Jun 2007; revised 9 Aug 2007; accepted 13 Aug 2007; published 15 Aug 2007

of product of the diffusion coefficient of particles and the squared wavenumber of probe light) for the particle suspension used is found to be 0.018 seconds.

The static layer is made of a poly(vinyl alcohol) (PVA) gel with polystyrene particles. In the past, PVA has been used to produce elastic [10] or viscoelastic [11] gels as optical tissue phantoms. The advantage of PVA is its solubility in water, so we can make phantoms of known scattering and absorption properties by adding polystyrene spheres and water-soluble dyes before gelation.

Solid phantoms of PVA gel are made by adding sodium borate (Borax, $Na_2B_4O_7.10H_2O$) as a cross-linking agent to an aqueous PVA solution. For this at first a PVA (Aldrich chemical company Inc, 99+% hydrolyzed) solution of 4% (by weight) in water is prepared. Another solution of 4% (by weight) of borax in water is prepared. Polystyrene particles and Ecoline black are added to this solution to make the desired scattering and absorption properties. Then this solution is mixed with a mixing ratio Borax/PVA of 20%. PVA gel when mixed with Borax is optically transparent. So the phantom will only show the properties of the particles and ink added. It is tested that the static and dynamic scattering phantoms have the same optical properties by total attenuation measurement. A glass cuvette of $2.5cm^3$ is used as a sample holder for dynamic phantoms. The static phantom is placed in between two thin glass slides (150 microns) and the thickness is exactly defined by placing two spacers of known thickness between the glass slides. The thicknesses of static phantoms used are 0.25, 0.5, 1.0, 1.5 and 2.0mm excluding the glass layer. The static phantom is placed on a frame which is attached to a linear translational stage and is placed on top of the dynamic scattering phantom.

The optical set up consists of a simple reflection mode configuration in which we illuminate the medium with laser beam perpendicular to the phantom surface, and collect the back-scattered photons using a lens and photoreceiver. A linearly polarized Uniphase 1125P He-Ne laser, of 632.8nm, with output power of 5mW is used as the source. A beam expander made of two positive lenses of focal length 20 and 30mm respectively is used to vary the beam diameter. The second lens is moved with respect to the other to obtain a change in beam diameter. It was measured with a commercial beam profiler that the beam diameter (e^{-2}) at the position of the sample surface can be obtained in a range of 0.5 mm to 4.0mm by translating the lens 2 in the direction of the beam. A lens (f =30mm) is placed at a distance of 25cm from the sample to collect the back-scattered light, with a photoreceiver on focus. Detection is performed with a New Focus (model 2001) photoreceiver, with an effective detector area of $0.81mm^2$. The AC signal is amplified by 40 dB and then applied to an anti-aliasing low-pass filter (5th order sampled capacitor Butterworth, f_c=20 kHz). The filtered signal is then applied to a 12-bit analogue to digital converter (National instruments, model AT-MIO-16E-10) where it is sampled at 40 kHz.

3.1. Monte Carlo simulation and coherence area computation

In the Monte Carlo simulation the scattering phantom is defined as a two-dimensional system. A collimated Gaussian beam of 632.8 nm with varying beam diameter is used as the source and is positioned perpendicular to the interface of the medium. A multilayer system is defined as used in the experimental set up, with the same optical properties including the glass layers. The thickness of the static layer is varied in steps, as in the experiments. The dynamic layer is defined with particles undergoing random motion, to tag photons having penetrated to this layer. Each simulation consists of 90000 detected photons. The detected photons are then separated to get two fractions: one from the static layer and one from the dynamic layer. This is done by separating Doppler-shifted and non-shifted photons. With the intensity distributions of these two fractions of photons the field correlation coefficients of statically scattered photons and dynamically scattered photons, and consequently the fractional coherence areas A_{coh}^{01} and A_{coh}^{11} can be calculated. By applying these values and fractions of non-Doppler shifted and Doppler shifted photons f_0 and f_1 in Eq. (4) we can calculate the modulation depth of the signal which is equal to M_0/DC^2.

#83991 - $15.00 USD Received 11 Jun 2007; revised 9 Aug 2007; accepted 13 Aug 2007; published 15 Aug 2007

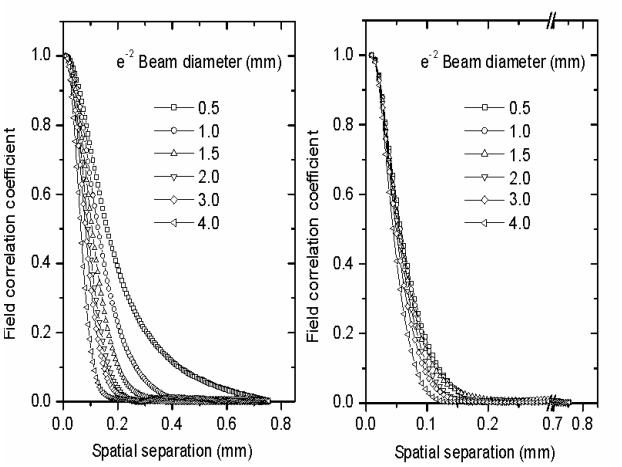

Fig. 3. Field correlation coefficients as a function of beam diameter for a two layered medium with a static layer of 0.5mm and a dynamic layer of 20mm. Left: field correlation coefficient γ_{EE}^{0} of non-Doppler shifted photons γ_{EE}^{1} Right: of Doppler shifted photons (note the different horizontal scales).

4. Results and discussion

Figure 3 shows calculated spatial field correlation functions produced by two fractions of photons. To the left is the correlation function of photons that traveled only within a static top layer of 0.5mm thickness and hence are non-Doppler shifted. To the right is the correlation function formed by photons which traveled through the dynamic layer and have undergone a Doppler shift. The width of the correlation function is a qualitative measure of the average coherence area. It can be observed that the correlation function of the photons coming from the deep layer is narrow compared to that from the static layer. This is because the photons coming from the deeper layer generate a wide intensity distribution on the surface of the medium, which is associated with smaller coherence areas. In contrast, photons from superficial statically scattering layer generate a narrow intensity distribution and large coherence areas as illustrated in Fig. 2. Furthermore, the width of the field correlation function of static photons is much more sensitive to beam diameter than the correlation function of Doppler photons: due to the larger amount of scattering events undergone by the Doppler shifted photons, their lateral distribution is much more governed by the optical properties of the medium than by the beam diameter.

#83991 - $15.00 USD Received 11 Jun 2007; revised 9 Aug 2007; accepted 13 Aug 2007; published 15 Aug 2007

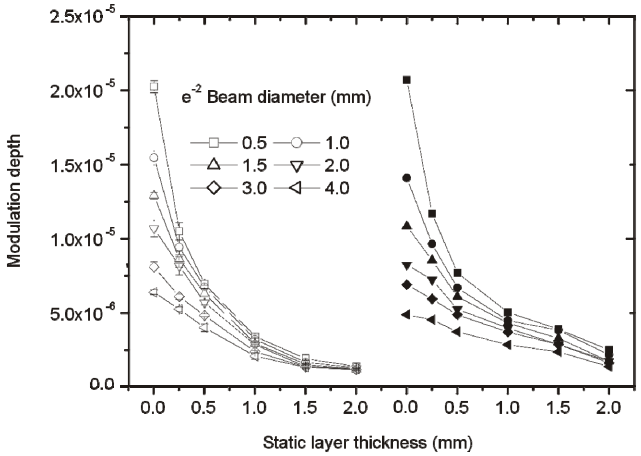

Fig. 4. Plot of modulation depth of a particle suspension for various thicknesses of static top layer. Left: measurement (Error bar represents standard deviation, error is very small); Right: simulation.

Figure 4 shows the signal modulation depth for different thicknesses of the static layer, from experiments (*left*) and from theoretical prediction using Eq. (4), (*right)*. Here the modulation depth as a function of the static layer thickness defines the depth sensitivity of the instrument, which is the sensitivity of the instrument to motion vs the depth at which motion occurs. As expected, it is observed that, as the thickness of the static layer increases the modulation depth decreases. However, this trend is suppressed with increasing beam diameter. For the narrowest beam the signal modulation ratio for motion at 0 and 0.5 mm depth, respectively, is 2.9. But for a wide beam (4.0mm) this ratio is reduced to 1.6. This shows that a narrow beam is more sensitive to scattering from superficial layers compared to a wide beam, while the sensitivity to motion at large depth is much less dependent on beam diameter. Measurements performed with a narrow beam will be very sensitive to changes in number of coherence areas with depth. In contrast, a wide beam which itself results in a wide intensity distribution of back scattered light and large number of coherence areas suppresses the depth related changes in the amount of coherence areas. This difference must completely be attributed to the effect of speckles, since the statistics of the photon penetration depth will be independent of beam diameter.

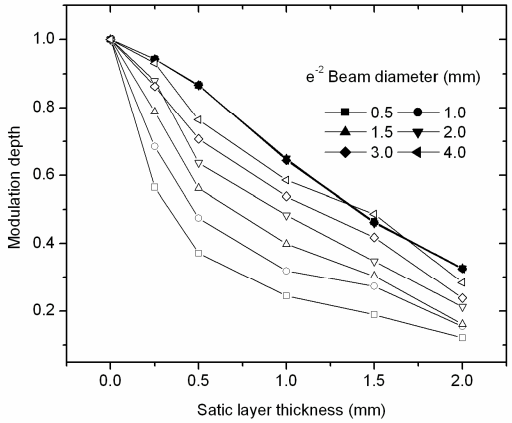

Fig. 5. Modulation depth (normalized to zero depth) vs static layer thickness with speckle effects (closed symbols) and without the speckle effects (shaded symbols, $A_{coh} = 1$).

#83991 - $15.00 USD Received 11 Jun 2007; revised 9 Aug 2007; accepted 13 Aug 2007; published 15 Aug 2007

The Monte Carlo simulated modulation depth (normalized to zero depth) vs static layer thickness with speckle effects (closed symbols) and without taking speckle effects [shaded symbols, by keeping $A_{coh}^{01} = A_{coh}^{11} = 1$ in Eq. (4)] into account for each beam diameter is shown as Fig. 5. The shaded symbols depict the data of Fig. 4 (right) without speckle effects, thus the modulation depth is only a function of the fraction of Doppler shifted and non-Doppler shifted photons and depends on photon penetration depth statistics alone. Consequently the modulation depth is equal for all beam diameters since the photon penetration depth is independent of beam diameter. Figure 5 shows that with speckle effects the signal modulation ratio for motion at 0 and 2.0 mm depth, respectively, is 8.33 for a beam of 0.5mm diameter. But for 4.0mm beam this ratio is only 3.57. When speckle effects are not taken in to account [Fig. 5 (shaded symbols)] the modulation ratio for motion at 0 and 2.0 mm depth is only 3.13 for all beam diameters. This trend clearly shows the effect of speckle phenomenon on the depth sensitivity of the instrument.

In Fig. 6 experimental modulation depth values are plotted against predicted values. It can be observed that for narrow beams (0.5 and 1.0 mm) and superficial layers (0 to 0.5 mm) the agreement between theoretical prediction and experimental results is within 10%. The variation is significant (up to 40%) for deeper layers because the signal-to-noise ratio in measurements is very low in these cases. Since the Monte Carlo detector is more sensitive and effectively collects very low amount of Doppler shifted light the measured modulation depth tends to saturate faster compared to the predicted results. This can be seen in Fig. 4 where for 1.5 to 2mm thickness the modulation depth is getting leveled off in measured result but not in the prediction.

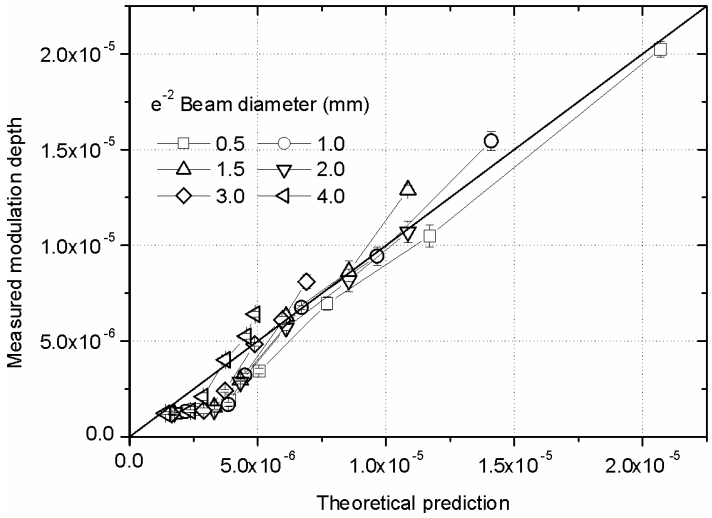

Fig. 6. Theoretical prediction vs measured modulation depth

5. Conclusion

Our results show that the depth sensitivity of the laser Doppler instrument is strongly influenced by coherence areas. A narrow beam is more sensitive to scattering in superficial layers than a wide beam due to the change of the average coherence area. Our earlier experimental study [3] showed that this beam diameter dependency will depend on the scattering level of the medium. A wide beam can be used to suppress the speckle effects and the sensitivity to scattering levels, but the modulation depth and lateral resolution will be compromised. The strength of the speckle effect on depth sensitivity will also depend on the scattering and absorption level of the tissue. The lower the level of the scattering and absorption the smaller the effect will be. This is because when scattering or absorption is high photons will travel shorter distances and leave the medium closer to the illuminating beam

#83991 - $15.00 USD Received 11 Jun 2007; revised 9 Aug 2007; accepted 13 Aug 2007; published 15 Aug 2007

making a narrow back-scattered intensity profile. So the effective coherence area will be larger and also the modulation depth. In this situation the LDPI flux signal will be very sensitive to the depth related changes in width of the intensity distribution and the resulting changes in the number of coherence areas.

Since our model proved to be correct it can be used to predict this sensitivity variation for different scattering and absorbing media. This is very relevant in LDPI applications were skin optical properties vary significantly in the region of interest and in time. For example during the uptake of certain drugs or in allergy tests [12] where the skin color changes, the optical properties of the skin vary which influences the signal response irrespective of the perfusion variation. Also in the case of a burn depth [5] or wound healing [6] assessment the changes in absorption and scattering by skin color or a grafted skin influences the measured perfusion signal, not only through the photon statistics, but also because of the speckle effects demonstrated here. Our theoretical model offers a valuable tool to predict the depth sensitivity and modulation depth changes in these complex situations.

In conclusion, the depth sensitivity of laser Doppler imagers as a function of tissue optical properties and illuminated beam diameter was assessed, both experimentally and theoretically. Our work shows that in scanning beam laser Doppler perfusion imagers a significant coherence area related cross talk will exist between the perfusion maps and the optical properties of the scanned tissue area, in particular for the contribution of superficial perfusion to the total perfusion map.

#83991 - $15.00 USD Received 11 Jun 2007; revised 9 Aug 2007; accepted 13 Aug 2007; published 15 Aug 2007